

Mechanical performance and corrosion behavior of TiAlSiN/WS₂ multilayer deposited by multi-plasma immersion ion implantation and deposition and magnetron sputtering

XIE Zhi-wen, WANG Lang-ping, WANG Xiao-feng, HUANG Lei, LU Yang, YAN Jiu-chun

State Key Laboratory of Advanced Welding and Joining, Harbin Institute of Technology, Harbin 150001, China

Received 10 May 2011; accepted 25 July 2011

Abstract: To reduce the friction coefficient of the superhard TiAlSiN composite coating, TiAlSiN/WS₂ multilayers were synthesized by multiple plasma immersion ion implantation and deposition as well as radio-frequency (RF) magnetron sputtering. X-ray diffraction (XRD), scanning electron microscopy (SEM), Raman spectrum, nano indentation, tribological and electrochemical tests were employed to characterize the microstructure, mechanical properties and corrosion behavior of the as-deposited multilayers. SEM results reveal that the TiAlSiN/WS₂ multilayers have a good periodicity. Nano indentation results show that the nanohardness of TiAlSiN/WS₂ multilayers is between that of the TiAlSiN and WS₂ coatings. Tribological tests prove that the friction coefficient of the TiAlSiN/WS₂ multilayers is lower and more stable than that of the TiAlSiN coating. In addition, the TiAlSiN/WS₂ multilayers show excellent corrosion resistance and the corrosion current density decreases obviously at a relative small modulation period.

Key words: TiAlSiN; WS₂; multilayer; friction coefficient; corrosion resistance

1 Introduction

In recent years, nanocomposite coatings (TiAlN, TiSiN and TiAlSiN) with hardness higher than 40 GPa have attracted extensive attentions because of their unique mechanical, chemical and wear properties [1–5]. Unfortunately, these coatings usually lack lubricating properties and exhibit a relatively high friction coefficients (0.6–1.0) at room or elevated temperatures [6–8]. Since a low friction coefficient can effectively reduce the contact temperature during the high speed and dry cutting process, nanocomposite coatings with super hardness and self-lubrication properties have great potential for improving the lifetime and the performance of cutting tools. Some researchers have mixed carbon into the composite coating and obtained a low friction coefficient [9–12].

Tungsten disulfide (WS₂) has been used widely in space applications due to its extremely low friction coefficient and long lifetime [13–14]. However, since the structure of tungsten disulfide (WS₂) is similar to that of molybdenum disulfide (MoS₂), its wear resistance deteriorates significantly when it is working in humid atmosphere [15–16]. Pervious study proposed that the

MoS₂/Ti multilayer structure was beneficial for increasing the resistance of the MoS₂ film to the moisture attack [17]. In order to reduce the friction coefficient of the TiAlSiN coating as well as increase the resistance to moisture atmosphere, TiAlSiN/WS₂ multilayer coatings were fabricated and their mechanical performance and corrosion behaviors were studied.

2 Experimental

Si (100) wafer and polished M2 (W18Cr4V) tool steel were used as substrates. Fabrication of the TiAlSiN/WS₂ coating was carried out in a multi-purpose plasma immersion ion implantation and deposition facility [18]. The TiAlSiN layer was fabricated by the multi-cathode plasma source using pure Ti (99.9%) and SiAl alloy (70%:30%, mass ration) cathodes. The WS₂ layer was obtained by the radio-frequency (RF) magnetron sputtering system. By controlling the working time of the multiple-cathode arc plasma source and the sputtering target, TiAlSiN/WS₂ multilayer coatings with various modulation periods were obtained. The parameters for synthesizing the TiAlSiN layer are displayed as follows: a pressure (N₂) of 0.3 Pa, a pulse bias voltage of 20 kV, a pulse repetition frequency of 50

Hz, a pulse bias voltage duration time of 60 μ s, a pulse duration time for the Ti cathode of 2 ms, a pulse duration time for the SiAl cathode of 2 ms. The WS₂ layer was deposited using the following parameters: a RF power of 600 W, a pressure (Ar) of 2 Pa, a bias voltage of 6 kV, a pulse repetition frequency of 100 Hz, a bias voltage duration time of 60 μ s. The further processing parameters for different multilayers are shown in Table 1.

Table 1 Processing parameters of different samples

Sample No.	Deposition time of each TiAlSiN layer/min	Deposition time of each WS ₂ layer/min	Modulation period/nm	Cycle
T0	–	240	–	1
S0	240	–	–	1
W1	5	10	100	24
W2	20	40	600	6

The crystalline structure of the films was determined by X-ray diffraction (XRD, Philips-X'pert) with Cu K α radiation, and the diffraction angle was scanned from 20° to 90°. A high-resolution field emission scanning electron microscope (SEM, FEI-Quanta-200) was used to study the cross sectional microstructure of the coatings. A MTS XP nano-indentation system was used to measure the nanohardness of the coatings in a mode of continuous stiffness measurement, and six indentations were conducted in each sample. The tribological properties were characterized by a ball-on-disc test with a load of 2 N on the sample through a 6.3 mm Si₃N₄ ball, and a line speed of 7.5 m/min was used during the test. The wear tracks of the coatings were observed by an optical microscope (OLYMPUS-PMG3). In addition, Raman spectroscopy was used to characterize the structure of wear tracks. Corrosion properties of all films were evaluated by the anode polarization curve tests in a saturated 3.5% NaCl solution with high purity graphite as the counter cathode, and a saturated calomel electrode (SCE) as reference electrode.

3 Results and discussion

3.1 Composition and microstructure

Figure 1 displays the XRD patterns of all samples. According to XRD results, the preferred orientation in the TiAlSiN coating is TiN(200). The coating in sample W1 also exhibits a TiN structure and no obvious WS₂ peak can be found. However, the coating in sample W2 exhibits a strong WS₂ peak and the intensity of TiN peak decreases greatly. This structural transformation of TiAlSiN/WS₂ multilayer may be attributed to the damage effect by a high energy ion implantation [17–18]. For

sample W1, because the WS₂ layer is very thin (<60 nm), high energy ion bombardment in the deposition process will change WS₂ to be an amorphous phase. However, since the coating in sample W2 has a thick WS₂ layer (>400 nm), high energy ion bombardment has negligible influence on the structure of WS₂. Consequently, a large intensity of WS₂ peaks can be found in sample W2.

Figure 2 presents the cross-sections of samples T0 and W1 on Si wafer. According to Fig. 2(a), the TiAlSiN

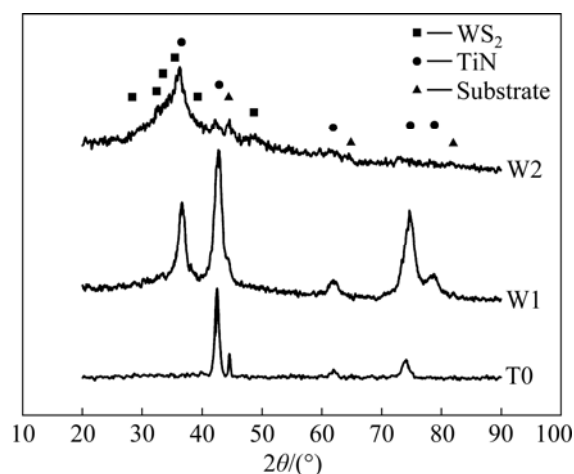


Fig. 1 XRD patterns of samples T0, W1 and W2

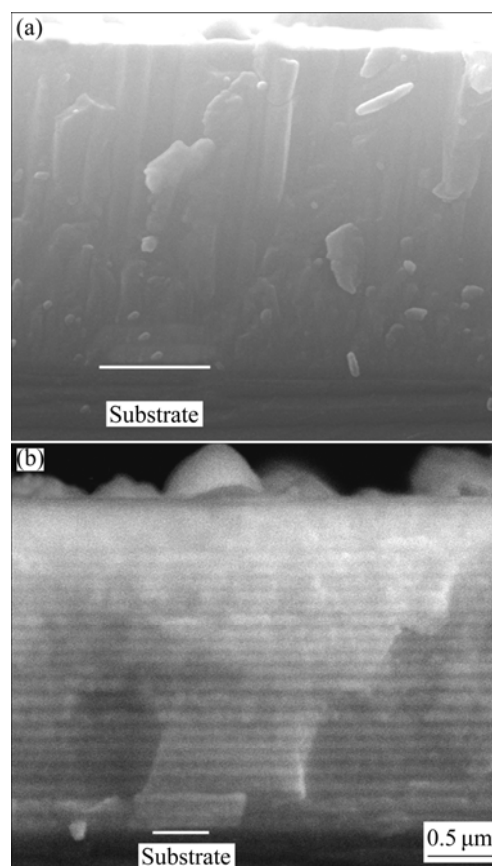


Fig. 2 SEM cross-sectional micrographs of samples T0 (a) and W1 (b)

coating shows a typical columnar structure. However, the cross section of the TiAlSiN/WS₂ multilayer shown in Fig. 2(b) exhibits an obvious layered structure formed in the coating. In addition, because a high energy ion implantation was applied during the layer deposition, the interface between adjacent layers was not very clear.

3.2 Mechanical properties

Figure 3 shows the nanohardness of all samples. The TiAlSiN coating (sample T0) has a high hardness of 35 GPa. The WS₂ coating has a low hardness of 5 GPa. The hardness of the TiAlSiN/WS₂ multilayer with the modulation period of 100 nm is about 16 GPa, and it decreases to 11 GPa as the modulation period increases to 600 nm.

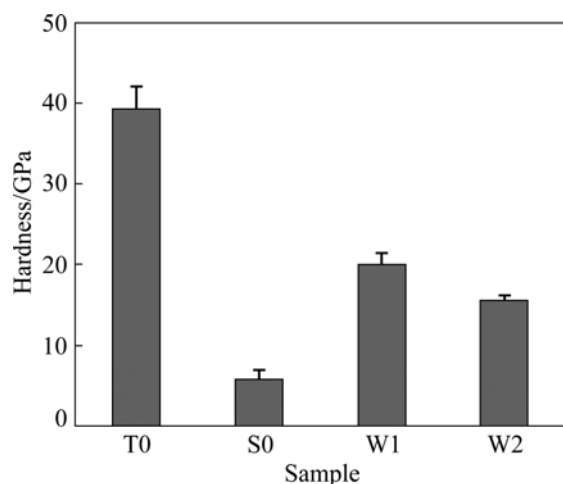


Fig. 3 Hardness of all samples

Figure 4 shows the friction coefficient curves of all samples. The WS₂ coating exhibits excellent wear performance and its friction coefficient is about 0.11. The TiAlSiN coating shows a high friction coefficient of

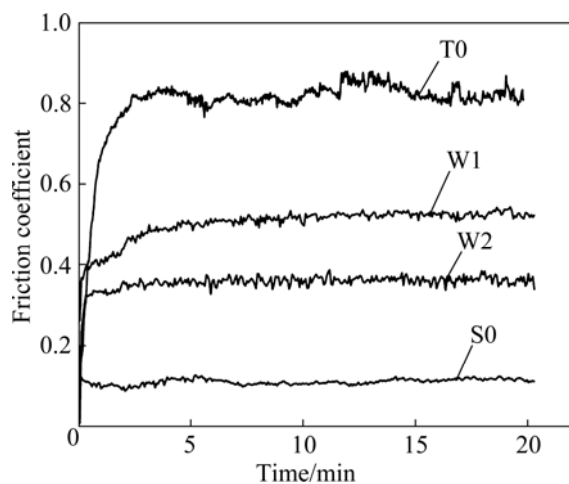


Fig. 4 Friction coefficient curves of all samples

about 0.82. The TiAlSiN/WS₂ multilayer coating exhibits an improved wear performance, and the friction coefficients of samples W1 and W2 are about 0.53 and 0.34, respectively, which is lower than that of the TiAlSiN coating.

Figure 5 shows the wear tracks of samples T0 and W1 as well as corresponding Si₃N₄ balls. According to Figs. 5(a) and 5(b), the width of the wear track in sample T0 is about 640 μm and the diameter of the wear track on the corresponding Si₃N₄ ball is about 650 μm. Figures 5(c) and 5(d) reveal that the width of the wear track is about 420 μm and the diameter of the wear track on the corresponding Si₃N₄ ball is about 450 μm. Comparing the friction curves and wear tracks of sample T0 with W1, it is clear that the TiAlSiN/WS₂ multilayer exhibits excellent wear performance and self-lubricating properties.

Figure 6 shows the Raman analysis for the wear track of sample W2. Peaks at 340, 410 and 550 cm⁻¹ prove the presence of WS₂ inside the wear track. However, WO₃ peaks at 650 and 801 cm⁻¹ also present inside the wear track, which should be deduced from the oxygen pollution during the deposition process. Based on the tribological and Raman results, the self-lubricating properties of the multilayers should be originated from the introduction of the WS₂.

Figure 7 shows the anode polarization curves of all samples. The corrosion current densities and corrosion potentials derived from these curves are listed in Table 2. It can be found that the corrosion current densities of samples W1 and W2 are lower than that of samples T0 and S0. Sample W1 with the modulation period of 100 nm possesses the lowest corrosion current density.

Table 2 Corrosion potentials and corrosion current densities

Sample	Corrosion potential/V	Current density/(A·cm ²)
T0	-0.707	4.378×10 ⁻⁴
S0	-0.721	5.323×10 ⁻⁴
W1	-0.685	5.972×10 ⁻⁵
W2	-0.703	3.635×10 ⁻⁴

Figure 8 exhibits the surface morphologies of samples T0, S0 and W1 after the anode polarization curve tests. It is obvious that a larger amount of big and deep corrosion pits are formed on the surfaces of samples T0 and S0. However, the surface of the sample W1 is smooth and few corrosion pits can be found. In accordance with the anode polarization curves and optical images, it can be found that the TiAlSiN/WS₂ multilayer coatings possess excellent corrosion resistance.

In general, the TiAlSiN coating possesses a columnar structure, which usually contains a lot of growth defects, such as holes and interstices. In addition, the WS₂ coating synthesized by magnetron sputtering has similar structure. Apparently, these growth defects and low surface density will provide corrosive channels and

eventually lead to the reduction of corrosive nature. However, the TiAlSiN/WS₂ multilayer coatings contain a lot of interfaces, which can effectively prevent the formation of columnar structure and large growth defects. Therefore, the TiAlSiN/WS₂ multilayer coatings possess excellent anti-corrosion properties.

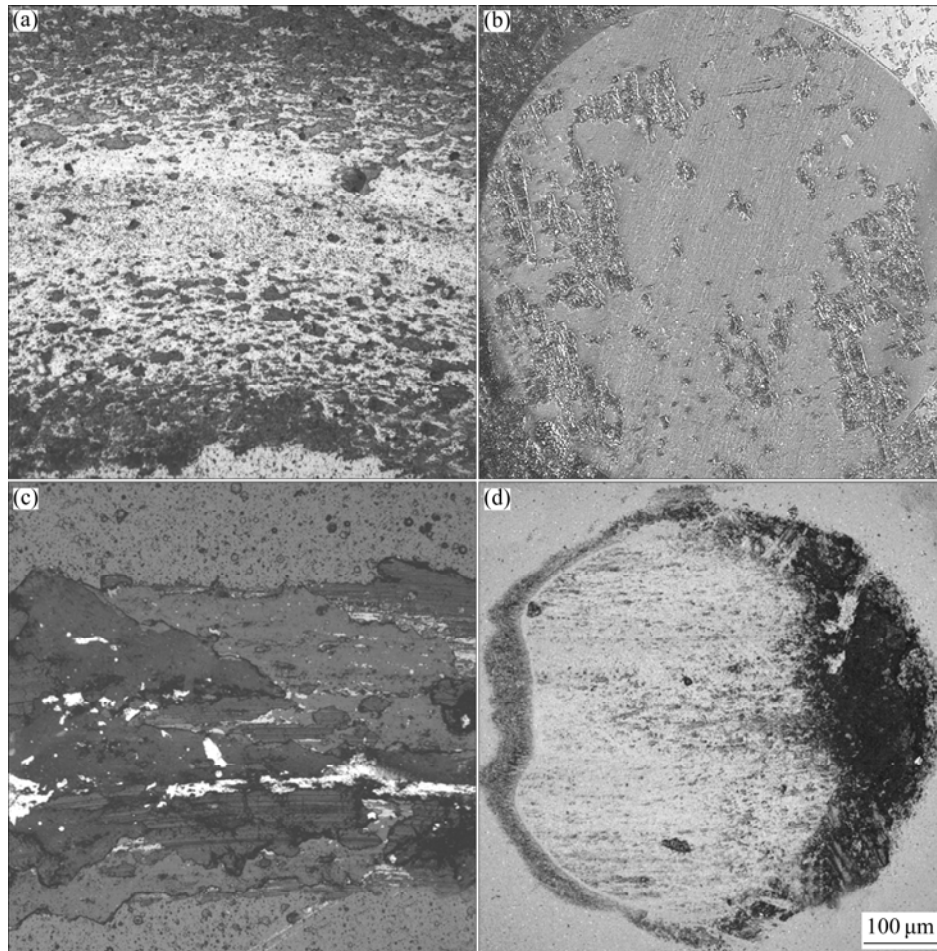


Fig. 5 Wear tracks of different samples after friction tests: (a) Sample T0; (b) Corresponding Si₃N₄ balls to sample T0; (c) Sample W1; (d) Corresponding Si₃N₄ ball to sample W1

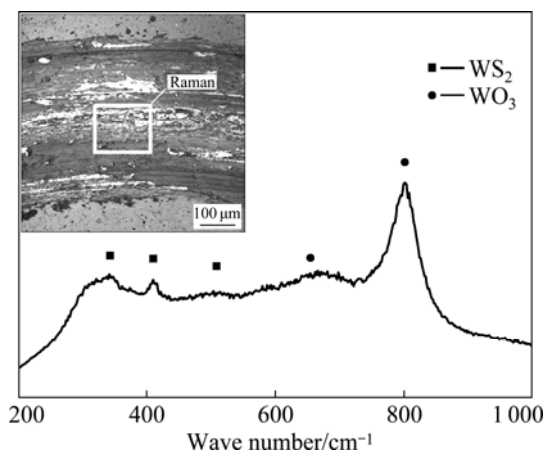


Fig. 6 Raman spectroscopy result inside wear track of sample W2

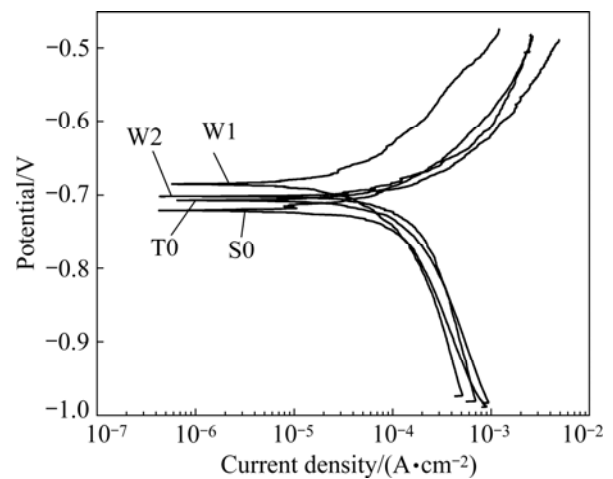


Fig. 7 Potential dynamic polarization curves of all samples

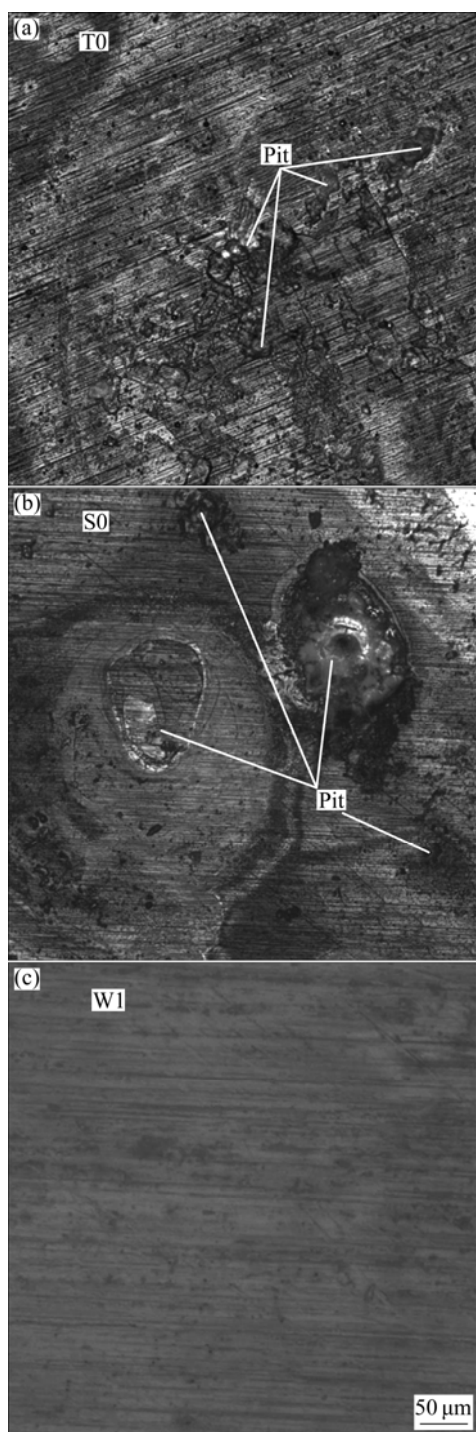


Fig. 8 Corrosion morphologies of samples T0 (a), S0 (b) and W1 (c)

4 Conclusions

1) The TiAlSiN/WS₂ multilayer coatings fabricated by multi plasma immersion ion implantation as well as the magnetron sputtering possess a typical layered structure.

2) The nanohardness and friction coefficient of TiAlSiN/WS₂ multilayer coatings are both between those

of the TiAlSiN and WS₂ coatings.

3) The TiAlSiN/WS₂ multilayer coatings present excellent corrosion resistances and the corrosion current density decreases with the modulation period.

Acknowledgements

The authors gratefully acknowledge the State Key Laboratory of Advanced Welding and Joining for financial support. The authors thank Dr. SUN Tao for helpful discussions and contributions during the hardness test.

References

- [1] VEPREK S, REIPRICH S, LI Shi-zhi. Superhard nanocrystalline composite materials: The TiN/Si₃N₄ system [J]. *Apply Physics Letters*, 1995, 66(20): 2640–2642.
- [2] VEPREK S, VEPREK-HEIJMAN M G J, KARVANKOVA P. Different approaches to superhard coatings and nanocomposites [J]. *Thin Solid Films*, 2005, 476(1): 1–29.
- [3] VEPREK S, ARGON A S. Mechanical properties of superhard nanocomposites [J]. *Surface and Coatings Technology*, 2001, 146–147: 175–182.
- [4] VEPREK S, VEPREK-HEIJMAN M G J. Industrial applications of superhard nanocomposite coatings [J]. *Surface and Coatings Technology*, 2008, 202(21): 5063–5073.
- [5] ZHANG R F, VEPREK S. On the spinodal nature of the phase segregation and formation of stable nanostructure in the Ti–Si–N system [J]. *Materials Science and Engineering A*, 2006, 424(1–2): 128–137.
- [6] YU Dong-hai, WANG Cheng-yong, CHENG Xiao-ling, ZHANG Feng-lin. Microstructure and properties of TiAlSiN coatings prepared by hybrid PVD technology [J]. *Thin Solid Films*, 2009, 517(17): 4950–4955.
- [7] CHANG C L, LEE J W, TSENG M D. Microstructure, corrosion and tribological behaviors of TiAlSiN coatings deposited by cathodic arc plasma deposition [J]. *Thin Solid Films*, 2009, 517(17): 5231–5236.
- [8] MA S, PROCHAZKA J, KARVANKOVA P. Comparative study of the tribological behaviour of superhard nanocomposite coatings nc-TiN/a-Si₃N₄ with TiN [J]. *Surface and Coatings Technology*, 2005, 194(1): 143–148.
- [9] MAYRHOFER P H, MITTERER C, HULTMAN L. Microstructural design of hard coatings [J]. *Progress in Materials Science*, 2006, 51(8): 1032–1114.
- [10] MA S L, MA D Y, GUO Y. Synthesis and characterization of super hard, self-lubricating Ti-Si-C-N nanocomposite coatings [J]. *Acta Materialia*, 2007, 55(18): 6350–6355.
- [11] JEON J H, CHOI S R, CHUNG W S. Synthesis and characterization of quaternary Ti-Si-C-N coatings prepared by a hybrid deposition technique [J]. *Surface and Coatings Technology*, 2004, 188–189: 415–419.
- [12] ABRAHAM S, CHOI E Y, KANG N. Microstructure and mechanical properties of Ti-Si-C-N films synthesized by plasma-enhanced chemical vapor deposition [J]. *Surface and Coatings Technology*, 2007, 202(4–7): 915–919.
- [13] RAI A K, BHATTACHARYA R S, ZABINSKI J S. A comparison of the wear life of as-deposited and ion-irradiated WS₂ coatings [J]. *Surface and Coatings Technology*, 1997, 92(1–2): 120–128.
- [14] WATANABE S, NOSHIRO J, MIYAKE S. Tribological characteristics of WS₂/MoS₂ solid lubricating multilayer films [J]. *Surface and Coatings Technology*, 2004, 183(1): 347–351.

- [15] SIMMONDS M C, SAVAN A. Structural, morphological, chemical and tribological investigations of sputter deposited MoS₂/metal multilayer coatings [J]. Surface and Coatings Technology, 1998, 108–109: 340–344.
- [16] ZHENG X H, TU J P, LAI D M. Microstructure and tribological behavior of WS₂-Ag composite films deposited by RF magnetron sputtering [J]. Thin Solid Films, 2008, 516(16): 5404–5408.
- [17] WANG Lang-ping, ZHAO Shao-wei, XIE Zhi-wen. MoS₂/Ti multilayer deposited on 2Cr13 substrate by PIID [J]. Nuclear Instruments and Methods in Physics Research Section B, 2008, 266(5): 730–733.
- [18] WANG Lang-ping, HUANG Lei, XIE Zhi-wen. Fourth-generation plasma immersion ion implantation and deposition facility for hybrid surface modification layer fabrication [J]. Review of Scientific Instruments, 2008, 79(2): 023306.

多元等离子体浸没离子注入与沉积和磁控溅射技术制备 TiAlSiN/WS₂多层薄膜的力学性能和腐蚀行为

解志文, 王浪平, 王小峰, 黄磊, 陆洋, 闫久春

哈尔滨工业大学 先进焊接与连接国家重点实验室, 哈尔滨 150001

摘要: 为了降低超硬 TiAlSiN 复合涂层的摩擦因数, 采用多元等离子体浸没离子注入与沉积和射频(RF)磁控溅射技术制备 TiAlSiN/WS₂ 多层薄膜, 利用 XRD、SEM、Raman 光谱、纳米探针、摩擦和电化学试验对薄膜的微结构、力学性能和腐蚀行为进行测试与分析。SEM 结果表明: TiAlSiN/WS₂ 多层薄膜具有清晰的调制周期。纳米硬度结果表明, TiAlSiN/WS₂ 多层薄膜硬度介于 TiAlSiN 和 WS₂ 涂层硬度之间。摩擦实验结果证实 TiAlSiN/WS₂ 多层薄膜的摩擦因数低于 TiAlSiN 涂层的, 且摩擦过程平稳。此外, TiAlSiN/WS₂ 多层薄膜表现出良好的抗腐蚀能力, 在相对较小的调制周期内, 其腐蚀电流密度显著降低。

关键词: TiAlSiN; WS₂; 多层膜; 摩擦因数; 抗腐蚀

(Edited by YUAN Sai-qian)